Residual Stress Characterization in MEMS Microbridges using Micro-Raman Spectroscopy

L.A. Starman Jr.*, E.M. Ochoa*, J.A. Lott*, M.S. Amer***, W.D. Cowan**, and J.D. Busbee**

* Air Force Institute of Technology, Lavern.Starman@afit.edu, Wright-Patterson AFB, OH 45433
** Air Force Research Laboratory, Wright-Patterson AFB, OH 45433
*** Wright State University, Dayton, OH, 45435

ABSTRACT

We characterize and measure the pre-released residual stress levels in polysilicon Micro-Electro-Mechanical Systems (MEMS) microbridges using micro-Raman spectroscopy. Raman spectroscopy is nondestructive, fast, and provides the potential for *in situ* stress monitoring during fabrication. Residual stress from the deposition process can have profound affects on the functionality and reliability of MEMS devices. Several post-fabrication processes are available (ion implantation, diffusion, and anneals) which can influence the residual stress in thin films. We performed a series of phosphorous implants to quantify the influence of doping and anneals on the residual stress levels in MEMS devices. This experiment demonstrates the effective use of Raman spectroscopy to monitor and provide information to help control or influence the residual stress in MEMS structures [1-4].

Keywords: Raman spectroscopy, MEMS, MUMPs, Residual stress, stress characterization.

1 INTRODUCTION

MEMS devices are used in many applications ranging from air bag triggers in automotive applications to chemical sensors in biomedical applications. However, due to the small size of MEMS devices, residual stresses can play a major role in the successful operation and reliability of devices. In order to obtain robust and reliable micromechanical devices, it is essential to understand how processing parameters affect the mechanical properties of thin-film layers used in MEMS devices. The mechanical properties of the structural layers, in particular the stress and stress gradients, are very important for device performance. Residual stress often causes device failure due to curling, buckling, or fracture. There are several post-fabrication processes which can influence the residual stress of MEMS devices prior to release. The processes presented here include post-fabrication annealing and ion implant doping. Through the use of micro-Raman spectroscopy, residual and induced stress profiles for MEMS structures can be obtained [1-3]. Since it is an optical technique, micro-Raman spectroscopy shows promise as a minimally invasive *in situ* measurement technique for the manufacture of MEMS devices.

2 Modelling

To determine the approximate post implant anneal times for maximum dopant uniformity, a TSUPREM model of the MUMPs fabrication process was created. TSUPREM is a microelectronics fabrication simulation tool used to model semiconductor fabrication processes [5]. TSUPREM simulations indicate phosphorous outgassing occurs during the post-processing high temperature anneals which inhibits dopant uniformity. A simulated 50 Å-thick oxide cap nearly eliminates the phosphorous outgassing. Figure 1 is a TSUPREM representation of the 1E16 $ions/cm^2$ phosphorous implant for a 10 μm-wide Poly1 beam. The simulation phosphorous dopant uniformity is significantly improved by the combined phosphorous implant, oxidation, and accompanying anneals.

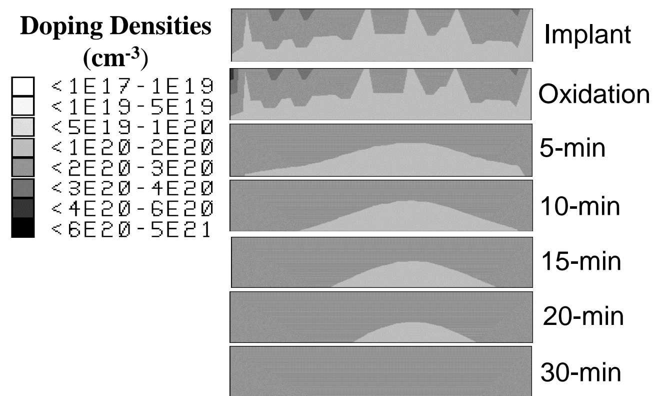

Figure 1: TSUPREM cross-section simulation of the 200 keV phosphorous implant (1E16 $ions/cm^2$ dose) with associated post implant anneal times for a Poly1 10 μm-wide beam.

3 EXPERIMENTAL

Raman spectra was obtained using a Renishaw system 2000 Raman microscope in backscattering mode.

The laser used is an Ar^+ laser at 514.5 nm. The laser power was limited to 2.4 mW to minimize sample heating. The MUMPs polysilicon structures studied here are 100 μm-long by 10 μm wide Poly1 microbridges as fabricated using MUMPs [6]. All test structures are anchored at each end to a silicon nitride layer. The Poly1 beams are suspended 2 μm above the substrate while Poly2 beams are 2.75 μm above the substrate. Figure 2a is a side-view of a Poly1 beam and Figure 2b is a scanning electron microscope (SEM) image of the polysilicon beams used in our implant experiments.

In the MUMPs process, the Poly1 and Poly2 structural layers are phosphorous doped by diffusion from the surrounding phosphosilicate glass (PSG) sacrificial layer. This dopin[illegible] nonuniform doping profile wh[illegible]ents. To in- c[illegible] stress gradi- e[illegible]nplants were p[illegible]n with doses o[illegible]$/cm^2$. For a 200 keV implant, t[illegible]ation level is located at a depth [illegible] Å.

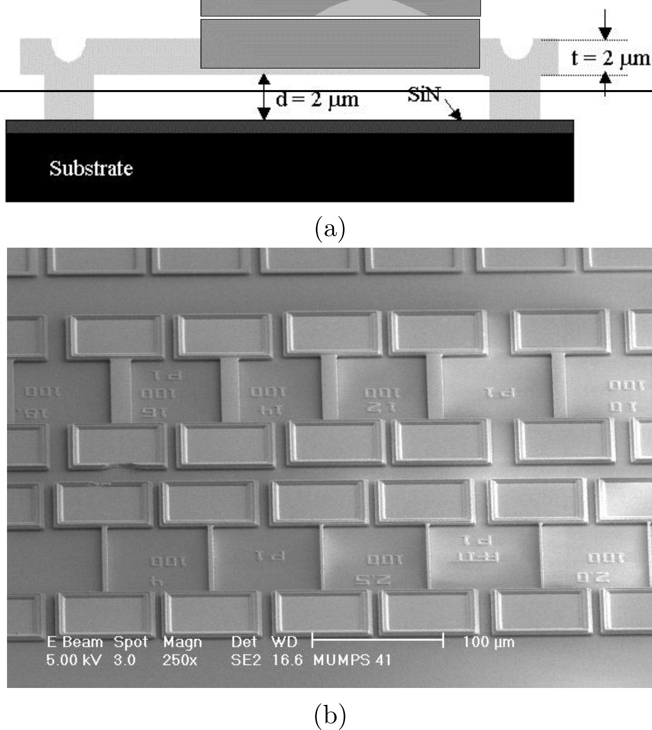

(a)

(b)

Figure 2: Polysilicon microbridge: (a) Side-view of a Poly1 microbridge, (b) SEM image of the microbridges of varying widths used in the implant study.

Since the foundry removes the second oxide through a partial etch to reduce stringers, thus exposing both Poly1 and Poly2 structures, an oxidation was performed prior to the 1100^oC anneals to minimize the phosphorous outgassing predicted by TSUPREM simulations. We performed a dry oxidation at 900^oC for 60-min on all sample die to grow the oxide cap on the exposed polysilicon surfaces. The oxide cap was measured using a surface profilometer to be approximately 655 Å-thick. All sample die were then simultaneously annealed at 1100^oC for 15-min. At this anneal temperature, the phosphorous dopant will diffuse thus increasing the overall dopant uniformity. Also, the polysilicon grain size will increase and aid in residual stress reduction [7-8]. Resistivity measurements performed on the implanted samples confirm that doping densities match the levels predicted by TSUPREM simulations.

4 RESULTS

The quantitative Raman stress profiles presented in Figures 3 and 4 are computed using our experimentally measured value of the phonon deformation potentials for Poly1 and Poly2 under hydrostatic pressure [9]. The strain dependence values obtained and used in creating the stress profiles for Poly1 and Poly2 were 2.19 cm^{-1}/GPa and 2.61 cm^{-1}/GPa respectively.

Figure 3 shows the Poly1 residual stress profiles obtained from micro-Raman spectroscopy for unreleased 10 μm-wide by 100 μm-long microbridges following the phosphorous implants and the 15-min 1100^oC anneal. Each residual stress profile depicts a different implant dose and is the average of three repeated micro-Raman scans on the same beam. As illustrated in Figure 3, the compressive residual stress has been reduced in the low dose implants (5E15 and 1E16 $ions/cm^2$) where the stress level approaches 0 MPa. In the higher implant doses (3E16, 5E16, and 1E17 $ions/cm^2$), the residual stress shifts from a compressive (less than 0 MPa) to a tensile stress (greater than 0 MPa) and steadily increases as the implant dose is increased. Since the polysilicon grain size is similar in all die due to the identical anneal times, the variation in measured stress profiles is due solely to foundry process variations between MEMS die and the increased dopant concentration in the beams.

Figure 4 shows the residual stress profiles obtained from unreleased 10 μm-wide by 100 μm-long Poly2 microbridges following the phosphorous implants and the 15-min 1100^oC anneal. Like the Poly1 structural layer illustrated in Figure 3, the low dose implants exhibit a compressive residual stress reduction in the Poly2 layer. Likewise, as the phosphorous implant dose increases, the compressive residual stress shifts to a tensile stress and steadily increases with higher implant doses.

On each MUMPs die, a set of test structures (Poly1 and Poly2 buckling beam arrays [10] and comb drive resonators [11]) are used to enable material properties characterization for each mechanical layer. The comb resonators are used to determine Young's modulus for each polysilicon layer. The resonant frequency measured

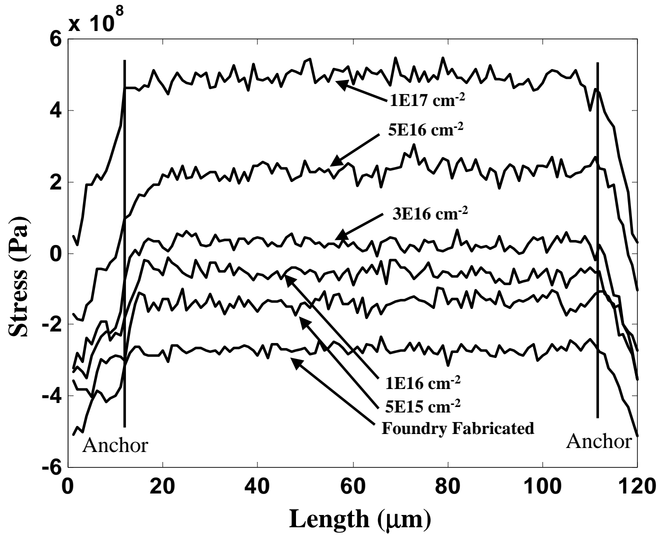

Figure 3: Poly1 residual stress profiles measured using micro-Raman spectroscopy for 100 μm-long by 10 μm-wide unreleased beams following the phosphorous implants and a 15-min 1100^oC anneal.

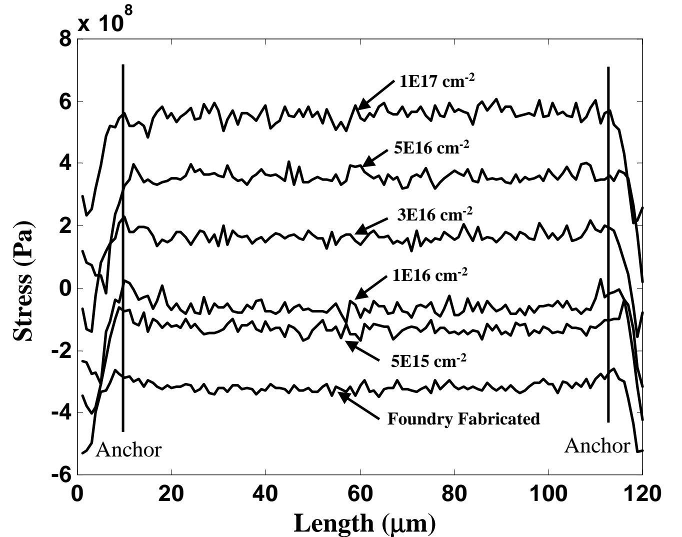

Figure 4: Poly2 residual stress profiles measured using micro-Raman spectroscopy for 100 μm-long by 10 μm-wide unreleased beams following the phosphorous implants and a 15-min 1100^oC anneal.

for Poly1 resonators was 22.59 kHz which corresponds to a Young's modulus of 129.38 GPa. The Poly2 resonance measured 18.94 kHz which gives a Young's modulus of approximately 163 GPa. The buckling beam arrays and comb-resonators allow for the quantitative measurements of residual stress following each implant and anneal once the die are released. We release the structures in HF, rinse in methanol, and then perform supercritical CO_2 drying.

The interferometric microscope (IFM) buckling beam arrays shown in Figure 5 demonstrate residual stress reduction is achieved by performing a phosphorous implant and a 15-min 1100^oC anneal. Figure 5a illustrates the critical buckling lengths of the MUMPs foundry fabrication for both Poly1 (top) and Poly2 (bottom) structural layers. From the critical buckling lengths and the measured Young's modulus for each layer, the residual stress level can be determined.

From Figure 5a, the Poly1 and Poly2 critical buckling lengths of 510 μm and 290 μm correspond to residual stress values of -6.927 MPa and -14.325 MPa respectively. In Figure 5b, after a 200 keV, 5E15 $ions/cm^2$ phosphorous implant and 15-min 1100^oC anneal. the Poly1 and Poly2 critical buckling lengths are both 860 μm. These buckling lengths correlate to residual stress values of -2.436 MPa and -1.629 MPa respectively. In Figure 5c after a 200 keV, 1E16 $ions/cm^2$ phosphorous implant with a 15-min 1100^oC anneal, the Poly1 and Poly2 critical buckling lengths are both $>$ 900 μm corresponding to residual stress values of $>$ -2.224 MPa for Poly1 and $>$ -1.487 MPa for Poly2. The Raman measurements suggest that residual stresses for this implant/anneal case are very near zero but still compressive. Other test structures on the die confirm that the polysilicon layers are not yet tensile.

Through IFM images and Raman spectra, the 1E16 $ions/cm^2$ phosphorous implant provides the minimal residual stress levels. The observed IFM images of the buckling beam arrays correlate well with the residual stress profiles obtained using micro-Raman spectroscopy for unreleased MEMS microbridges in low dose implant cases. For higher implant doses, the maximum buckling beam array lengths become significantly shorter. In the Raman stress profiles shown in Figures 3 and 4, higher implant doses result in tensile stress. Buckling beams should not buckle if they exhibit a true tensile stress. A possible reason for this result is the MUMPs polysilicon is changed to a porous silicon in high dose phosphorous implants. Porous silicon will weaken the test array resulting in shorter buckling lengths. Additional experimentation is necessary to accurately correlate between the residual stress values from micro-Raman spectroscopy and the stress values obtained from buckling beam arrays for highly doped samples.

5 CONCLUSION

Through phosphorous implants and accompanying anneals, the inherent residual stress in MEMS structures can be reduced or altered. More importantly, through the use of micro-Raman spectroscopy, the residual stress of unreleased MEMS structures can be monitored. This monitoring tool coupled with straight forward processes to adjust residual stress values could be exploited to

vastly improve the yield, reliability, and functionality of MEMS devices. This work is sponsored by the Materials and Manufacturing Directorate, Air Force Research Laboratory, Wright-Patterson AFB, OH.

The views expressed in this article are those of the author and do not reflect the official policy or position of the United States Air Force, Department of Defense, or the US Government.

REFERENCES

[1] W. D. Cowan, "Materials impacts on Micro-Opto-Electro-Mechanical systems," SPIE-MOEMS and Miniaturized Systems, Santa Clara, CA., Vol 4178, pp. 30-41, 18-20 Sept 2000.

[2] L. Starman, J. Busbee, J. Reber, J. Lott, W. Cowan and N. Vandelli, "Stress measurement in MEMS devices," Technical Proceedings of the 4th Intl. Conf. on Modeling and Simulation of Microsystems, Hilton Head, SC 398-401, 2001.

[3] L.A. Starman Jr., J.A. Lott, M.S. Amer, W.D. Cowan and J.D. Busbee, "Stress reduction characterization using Raman spectroscopy measurements on MEMS devices," International Conference on Optical MEMS and their Applications, Busena Terrace, Okinawa, Japan, 24-28 Sept 2001.

[4] I. De Wolf, "Micro-Raman spectroscopy to study local mechanical stress in silicon integrated circuits," Semiconductor Science Technology, Vol. 11, 139-154, 1996.

[5] TSUPREM-4 User's Manual, Technology Modeling Associates, Inc., 3950 Fabian Way, Palo alto, CA 94303, 1993.

[6] D.A. Koester, R. Mahadevan, B. Hardy and K. W. Markus, $MUMPs^{TM}$ Design Handbook Rev. 5, Cronos Integrated Microsystems, 3021 Cornwallis Road, Research Triangle Park, NC 27709, 1999.

[7] D. Maier-Schneider, A. Köprülülü, S. Ballhausen Holm and E. Obermeier, "Elastic properties and microstructure of LPCVD polysilicon films," Journal of Micromechanical Microengineering, Vol. 6, 436-446, 1996.

[8] J. Singh, S. Chandra and A. Chand, "Strain studies in LPCVD polysilicon for surface micromachined devices," Sensors and Actuators, Vol. 77, 133-138, 1999.

[9] E. Anastassakis, A. Cantarere and M. Cardona, "Piezo-Raman measurements and anharmonic parameters in silicon and diamond," Physical Review B, Vol. 41, No. 11, 7529-7535, 1990.

[10] W. Fang and J. A. Wickert, "Post buckling of micromachined beams," Journal of Micromachanical Microengineering, Vol. 4, 116-122, 1994.

[11] W Chi-Keung Tang, "Electrostatic comb drive for resonant sensor and actuator applications," University of California, Berkeley, 1990.

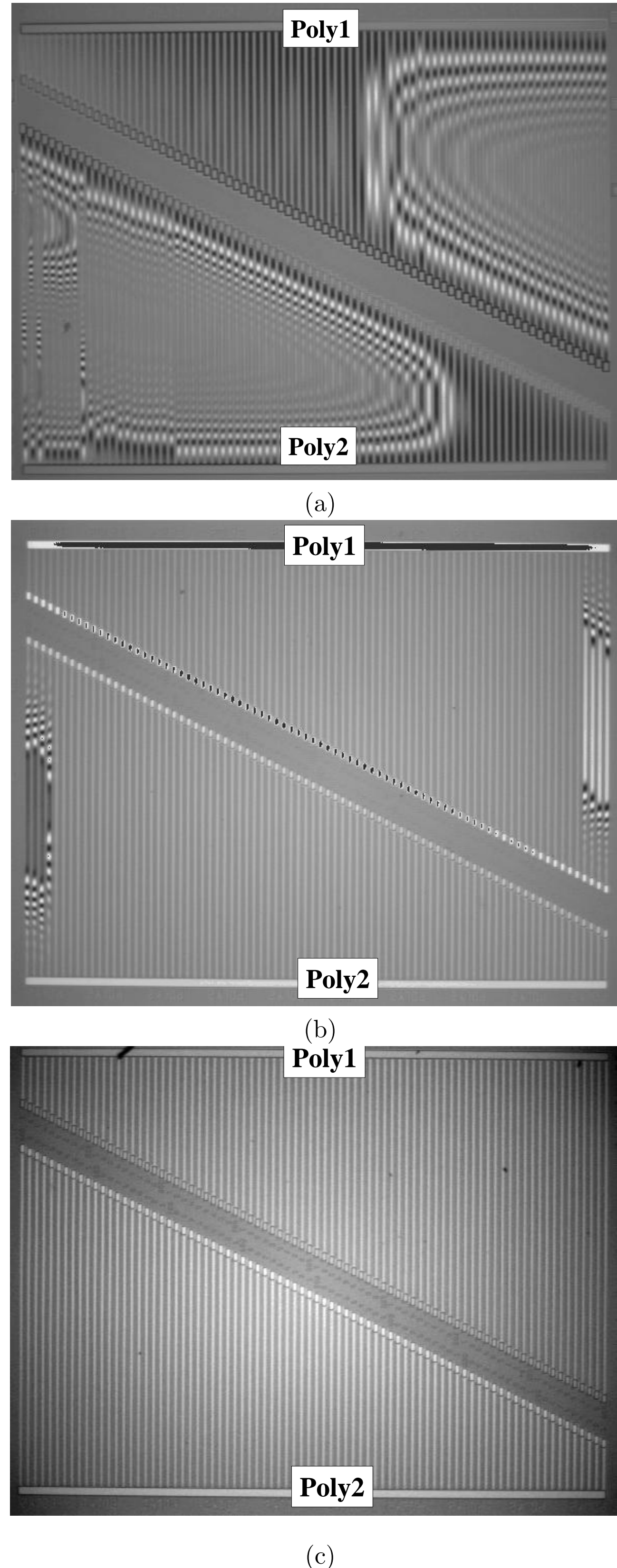

Figure 5: (a) Interferometric microscope (IFM) images of (a) Foundry fabricated Poly1 (top) and Poly2 (bottom) buckling beam arrays following release. (b) Poly1 (top) and Poly2 (bottom) buckling beam arrays following a 5E15 $ions/cm^2$ phosphorous implant, 15-min 1100^oC anneal, and HF release. (c) Poly1 (top) and Poly2 (bottom) buckling beam arrays following a 1E16 $ions/cm^2$ phosphorous implant, 15-min 1100^oC anneal, and HF release.